Kingdom of Saudi Arabia

Al-Imam Mohammad Ibn Saud Islamic University

College of Sciences

Department of Chemistry

ANODISING of ALUMINIUM

A graduation Project Improving Corrosion Resistance Properties of Aluminum by Anodic oxide film formation

by

Nasser Mohammed Al-Douaydi

Supervisor

Prof. **D**r. Mortaga Mohamed Abou-Krisha

Riyadh- KSA- MAYO. 2015

TABLE OF CONTENTS……...2
Abstract…… …...3

CHAPTER 1: INTRODUCTION……..4
1.1 Introduction……..…… …...4

CHAPTER 2: THEORETICAL BACKGROUND…….…….....6

2.1 *Review of Litrature*……..……..…6
2.2 Types of Oxide Films on Aluminum…….……6
2.3 *AAO Electrochemistry*…….....7
2.4 *Formation Mechanisms for Producing Barrier Layers and Nanoporous Alumina*…..9

CHAPTER 3: MATERIALS AND METHODS……..17
3.1 The relations (T-τ) and quantitative treatment of data.…….……...……....18

CHAPTER 4: RESULTS AND DISCUSSION……....22
4.1 The effect of electrolyte type……22
4.2 The effect of applied DC voltage…….…23
4.3 X-ray diffraction analysis……...…24
4.4 The anodic and cathodic behavior…….……25

CHAPTER 5: CONCLUSION ……..…….... 26

REFERENCES…….…….…….27-30

ABSTRACT

The anodization of aluminum is an electro-chemical process that changes the surface chemistry of the metal, via oxidation, to produce an anodic oxide layer. During this process a self organized, highly ordered array of cylindrical shaped pores can be produced with controllable pore diameters, periodicity and density distribution. This enables anodic aluminum oxide (AAO) to be used as templates in a variety of nanotechnology applications without the need for expensive lithographical techniques. Studies were performed to determine the effect of different factors on the properties and so the dissolution resistance of the anodic film of Al. Thermometric measurements were applied to evaluate the dissolution rate. The effect of electrolyte type using different acids and sodium carbonate on the corrosion resistance of AAO formed was studied and the obtained results show that the anodization in sulphuric acid was the best one. The applied DC voltages, in the presence of sodium carbonate solution (commercial low-cost salt compound), show a parallel increase in the dissolution resistance of studied Al in hydrochloric acid. The results show that films formed by sodium carbonate solution were of porous type and have pronounced corrosion resistance. Scanning electron microscope and x-ray diffraction further examined the films. The anodic and cathodic behavior and the effect of the scanning rate on the polarization of Al in sodium carbonate solution were studied.

CHAPTER 1
INTRODUCTION

1. Introduction

The anodization process of metals has been used by industry to protect metal components from corrosion for approximately 90 years. During this electro-chemical process the surface chemistry of the metal is changed, via oxidation, to produce an anodic oxide layer that is thick enough to stifle further oxidation. Aluminum metal (Al), because of its high strength to weight ratio, has found numerous engineering applications [1][2] and as early as the mid 1920s components on seaplanes used in aviation transportation were being anodized in chromic acid [3]. Two types of anodic Al oxide exist; the first is a non-porous barrier layer that is thin, hard, wear resistant and behaves as an electrical insulator. The second, a thicker porous oxide structure, is called the anodic aluminum oxide (AAO) layer. This layer structure has a high aspect ratio and consists of a porous structure. In engineering applications, this pore structure must be sealed to prevent corrosion. Oxide layers generated during anodization can also be produced on materials such as: magnesium (Mg), niobium (Nb), silicon (Si), tantalum (Ta), tin (Sn), titanium (Ti), tungsten (W), zinc (Zn) and zirconium (Zr).

In recent years, there has been a renewed interest in AAO layers for use as templates in a variety of nanotechnology applications. This is due to the highly controllable pore diameter and cylindrical shape, their periodicity and their density distribution. Using the conventional anodization process the arrangement of the pores is quite disordered, however Masuda *et al*. [4] in 1998, using a two-step anodization process was able to produce a highly ordered hexagonal pore structure from a set of pre-arranged macroscopic parameters. These controllable macroscopic parameters dictated the resulting nano scaled structure that is formed in the AAO layer, thus producing a nano array that can be used in a variety of nanotechnology applications.

In the last decade, there has been a veritable explosion of ideas for the potential applications of nano-structured materials. To date, almost all traditional methods of producing synthetic materials have been revisited and investigated for possible use in the manufacture of nanomaterials. Nanomaterials are materials with basic structural units, grains, particles, tubes, spheres, fibers or other

constituent components in the range of 0.1 nm to 100 nm. They are increasingly becoming the subject of many investigations in several fields such as materials science, biotechnology and biomedicine [5,6]. Nanomaterials can be made from a wide range of solid materials such as metals, ceramics, polymers, organic materials and composites. They can come in a wide range of morphologies namely spheres, rods, tubes and plates. In addition, these materials can be grown or self-assembled to replicate the dimensions of natural entities such as collagen fibers [7].

CHAPTER 2

THEORETICAL BACKGROUND

2.1 Review of Litrature

Al metal is a substantial component of the Earth‘s crust, (approximately 8%) but due to its reactivity with naturally occurring oxygen in the atmosphere, it is found in combination with other materials. It is a constituent of bauxite ore and it only became viable to process about 100 years ago. Following the pioneering work of Sir Humphrey Davy and physicist Hans Christian Oersted (who is credited with the manufacture of the first Al nodules), Karl Bayer was able to refine and improve the manufacturing of alumina from bauxite. Alumina (Al_2O_3) is the only known stable oxide of Al and contains 52.8% of the element by weight. Today, due to its wide applications, Al is the most produced non-ferrous metal [8].

2.2 Types of Oxide Films on Aluminum

Al is a reactive metal that reacts readily with the oxygen present in the atmosphere at ambient temperatures to create a thin amorphous nanometer (1–10 nm) oxide layer. The thickness of the oxide layer is temperature dependent and at temperatures above 500 °C, both amorphous and crystalline aluminas are present [9]. This layer has the advantage of preventing the further dissolution of the Al and thus provides an effective protective barrier. This is in direct contrast to the permeable oxide layer that is built up on ferrous metal surfaces; thus allowing further corrosion to continue. The protective oxide layer on the surface of Al has enabled this metal to be used in a variety of industrial applications [10]. This oxide layer is very important and the control of its morphology and surface features is critical to many applications. It was shown as early as 1935 by Verwey [11] and other researchers [12] that the anodic film will react further with the environment, resulting in hydration of the outer surface of the barrier film. Thus, the oxide structure consists of two distinct layers, a hydrated porous layer growing on top of a thin inert dense layer, normally called the barrier layer.

2.3 AAO Electrochemistry

To use Al effectively for a wide variety of applications means that the metal needs to be protected. Anodization of Al was first used on an industrial scale in the mid 1920s, since then the range of applications has steadily increased and accordingly the anodization process has been actively investigated and refined [13]. It is known that during the anodization process, Al produces a highly impervious protective layer on its surface. The anodic layer parameters such as barrier layer thickness, pore diameter and pore height are directly dependent upon the steady-state voltage used in the creation of the layer [14-17]. This is graphically presented in Figure 1, which also shows the results of varying both the voltage and the current on the surface of an Al sample. It can be seen that at low voltages and high currents, pitting at the crystallographic boundaries begins, while at higher voltages and lower currents, electro-polishing effects take place. As the voltage is further increased, the current decreases and a porous layer will form. And finally, at extremely low currents and high voltages, a thick layer of Al oxide is formed.

Figure 1. Anodic polarization of aluminum in different electrolyte solutions (reproduced from Reference [18]).

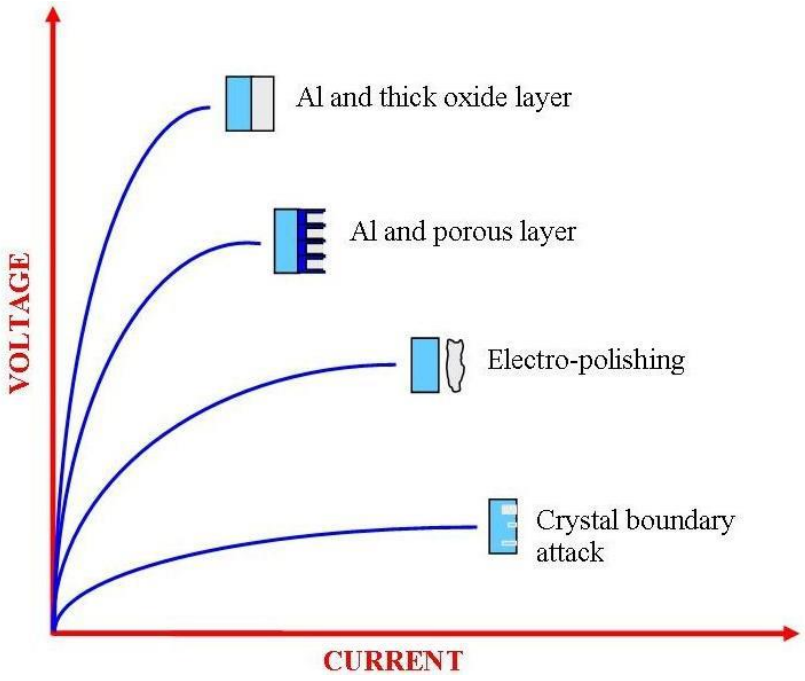

The advantage of using porous alumina as a template is that it enables selected nano-pore fabrication using general laboratory equipment, see Figure 2.

The proportionality of the cell size with respect to the electrochemical conditions allows one to macroscopically dictate the growth and final size of the pores manufactured. The equation is a simple one where an Al substrate is used with a particular acid to achieve nano-pores with an empirically derived set of electrochemical conditions. Al + acid + voltage = nano-pores Initially, the quality of the Al substrate, its surface structure and/or any surface pre-treatments will have a significant impact on the morphology and the resulting nano-structures formed on the substrate surface during the anodization process. To begin with, the Al substrate will have a pre-existing oxide layer over its surface, which is normally produced by the ambient oxygen in the atmosphere. In addition, the substrate could also have a pre-existing surface structure produced by a mechanical, thermal, chemical and electrochemical process. All of these surface treatments prior to anodization can have a significant impact on the self-ordering of the pore structures that form on the surface of the substrate during the anodization process. This is because the pore nucleation mechanism is a combination of both random nucleation and nucleation produced by the effects of surface defects, such as scratches, pits, impurities and grain boundaries. It should also be pointed out that during the anodization process, surface defects are favored sites for pore nucleation. Furthermore, studies have shown that the presence of alloying elements in the Al substrate not only tend to reduce the rate of growth of the forming oxide layer, but also influence the structure of the oxide layer during the anodization process [19].

Figure 2. Experimental equipment used to produce anodized aluminum oxide.

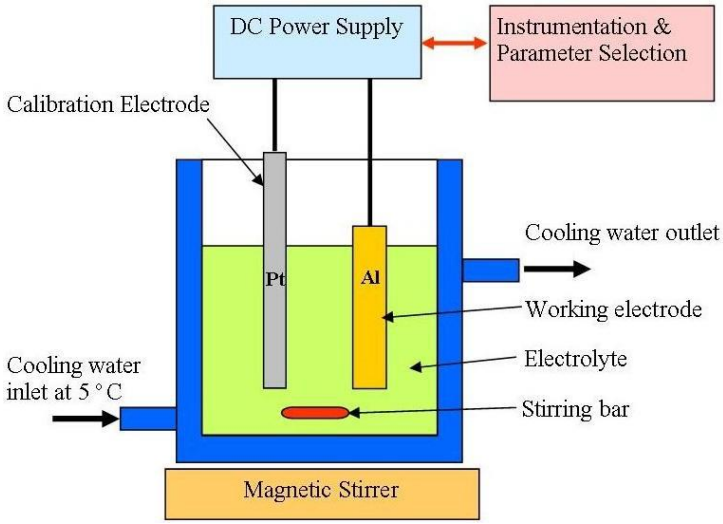

2.4 Formation Mechanisms for Producing Barrier Layers and Nanoporous Alumina

The formation of a thick porous oxide layer on Al has been extensively exploited by industry for many years to provide an effective surface finish or as a pre-treatment for further surface processing. However, it has only been the recent advances in nanotechnology and the need to manufacture one dimensional materials that have initiated a considerable renewed effort into understanding the mechanism underlying the formation of the nano-porous membrane and its dependence on several macroscopic parameters. Although the anodization of Al had been known for many years, it was Keller *et al.* who undertook the first detailed investigation of the actual mechanism behind pore nucleation and the formation of the porous oxide layer [14]. As mentioned earlier, there are two types of oxide that can be produced; the first is the barrier layer or film and the second is the nano-porous oxide layer. In both cases the oxide formation process is heavily governed by the pH of the electrolyte composition involved and the operating conditions used.

The non-porous barrier oxide layer is insoluble or dissolves at a slower rate than it is formed in the electrolyte. Generally, the electrolyte used is neutral or a basic solution with a pH greater than 7 [20]. Typical solutions that have been used are ammonium borate, phosphate and tartrate compositions. In addition, several organic acids such as citric, malic and glycolic have also been used. The barrier layer formed under these conditions is generally thin, non porous and rapidly forms under an applied voltage. The formation mechanism is straightforward and consists of two stages. In the first stage a constant current density is maintained, while the voltage increases linearly with time. To maintain the constant current density, the electric field strength must also be constant across the barrier layer, thus as the barrier layer grows the voltage increases until the formation voltage is reached. In the second stage the formation voltage is maintained while the barrier layer continues to grow by the migration of Al^{3+} ions outwards into the electrolyte and the inward motion of O^{2-} and OH^{-} ions [13], see Figure 3. The oxide formation occurs at both the metal/oxide and the oxide/electrolyte interfaces, with approximately 60% of the oxide growth occurring at the metal/oxide interface where the O^{2-} and OH^{-} ions combine with

the Al metal. The balance of the porous growth occurs at the oxide/electrolyte interface where the Al^{3+} ions react with the water molecules in the electrolyte. As the thickness of the barrier layer increases, the electrical resistance also increases, the metal/oxide and oxide/electrolyte interfaces remain planar and the current flow decreases with time. Towards the end of this stage the barrier layer has fully formed and remains constant. Thus, the growth layer has decreased to a point where it is equal to the rate of dissolution. During this process the Faradaic current efficiency in building the oxide layer is high, close to 100% [21]. In addition, the resulting barrier layer thickness is directly proportional to the applied voltage and is approximately 1.0 to 1.4 nm per volt. The formation of the oxide tends to produce a level surface, with any initial minor surface imperfections such as roughness being filled-in by the forming oxide. The resulting oxide thickness is generally uniform and any surface flaws in the metal surface tend to produce localized current concentrations that result in some increased thickening of the oxide. At the end of this anodization process the surface chemistry is stabilized and resists any further reactions with its environment. In addition, the resultant barrier layer is hard, wear resistant and behaves as an electrical insulator.

The formation process of the nano-porous oxide layer is a complex process that produces a self organized hexagonal pore array, these hexagonal honeycomb structures have been reported by several researcher‘s [4,22-28]. Unlike the barrier layer formation mentioned in the previous paragraph, the porous structure consists of a thin non porous oxide layer of constant thickness that is adjacent to the metal substrate that continually regenerates [29] at the base of the pore while the pore wall is being created, this wall increases in height with time. The particular electrolyte, its concentration, the anodic voltage and bath temperature are the main parameters in determining the pore size and the distance between pores.

Figure 3. Schematic of the major features involved in the formation of the barrier layer.

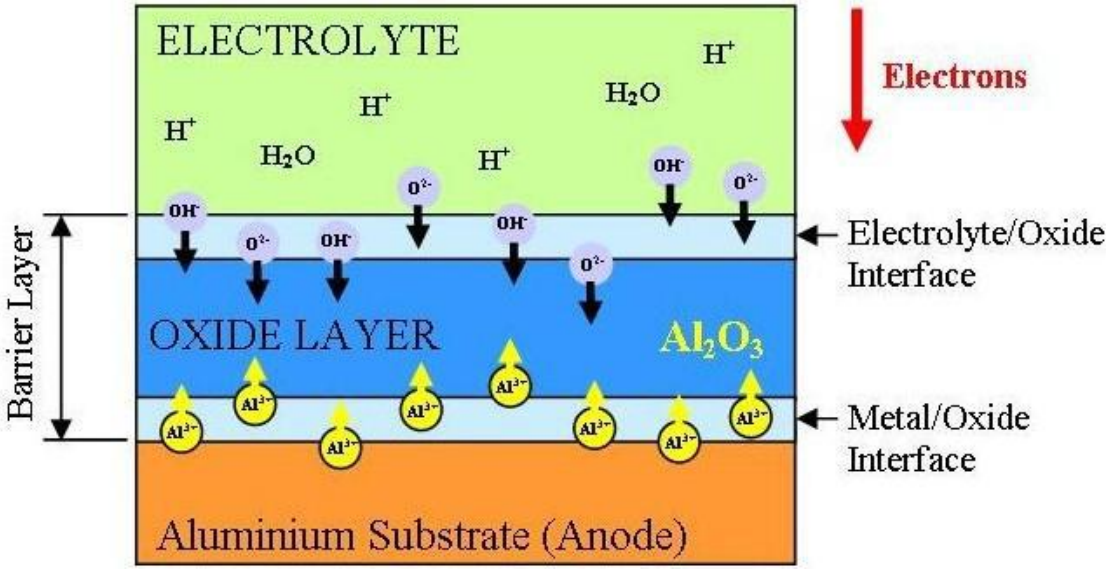

Typical electrolytes used to produce this type of oxide layer have a pH that is less than 5, and slowly dissolve the forming oxide layer. Examples of the acids used are sulfuric, phosphoric and oxalic. However; mixtures of organic and inorganic acids have also been used. The properties of the electrolyte are important in the formation of porosity and permeability. Electrolytes that are composed of less concentrated acids tend to produce oxide coatings that are harder, thicker, less porous and more wear resistant than those composed of higher concentrated acids[30]. But the most important factor that must be considered when forming the porous oxide is the electrolyte‘s ability to sustain a significant flow of Al^{3+} ions from the metal substrate into the electrolyte. There are two mechanisms that are responsible for the loss of Al^{3+} ions from the metal substrate. The first is by the direct expulsion of ions by the applied electrical field and the second is the dissolution of the forming oxide layer. In addition, if there are regions of high current flows when the electric field is applied, an increased dissolution rate can result (field assisted dissolution) [31].

The origin of pore nuclei and the exact mechanism of pore nucleation are still largely unknown. Several formation models have been proposed [31-33]; one model explains that pore nucleation results from an electric field assisted local chemical dissolution [34] at the electrolyte/oxide interface and oxide generation at the metal/oxide interface. This model explains that oxides formed using

electrolytes with a pH greater than 5 produces a barrier layer in which the Al^{3+} ions lost from the metal substrate are retained in the oxide layer. This layer has uniform thickness and is stable. However, for electrolytes with a pH less than 5, there is a significant flow of Al^{3+} ions into the electrolyte and as a consequence, there are regions where the formation of new oxide at the oxide/electrolyte interface is unstable. This regional instability produces variations in the applied electrical field; this in turn results in an increased dissolution rate [35,36]. This mechanism produces an underlying metal/oxide and oxide/electrolyte interfaces that consist of a large number of hemispherical depressions per cm^2 that corresponds to the pore density. In these depressions the electrical field tends to be more concentrated due to the focusing effect of the hemispherical shape, hence the increased dissolution rate. [37]. In contrast, the electrical field is fairly constant over the surface of the barrier layer formed in an electrolyte with a pH greater than 5, where the oxide thickness is uniform and stable. These hemispherical depressions form the foundations of the resulting pore structures. The location of these depressions is also influenced by the initial surface topography, surface imperfections such as impurities, pits, scratches, grain boundaries and surface treatments prior to anodization. Recently Patermarakis *et al.* [38] proposed a pore nucleation model that results from the spontaneous recrystallization of the unstable rare lattice of oxide formed at the surface of the Al adjacent to metal/oxide interface to a more stable denser nano-crystalline oxide located in the oxide layer. The resulting recrystallization ruptures in the surface and produces regions of rarefied oxide between nanocrystallites (anhydrous/amorphous). It is in these regions that pore nuclei form. Earlier studies by Habazaki *et al*. indicated the potential for the enrichment of alloying elements, dopants and/or impurities in the Al substrate adjacent to the metal/oxide interface [39]. The enrichment layers were found to be about 1 to 5 nm thick immediately beneath the metal/oxide interface and were a consequence of the oxide growth. These enrichment layers may also be involved in the initiation of changes within the oxide layer that promote pore nucleation. In a recent investigation by Zaraska *et al*. the presence of alloying elements in an Al alloy (AA1050) not only slowed the rate of oxide growth, but also influenced structural features such as porosity, barrier layer thickness, pore diameter and pore density of the forming oxide layer

[19]. In the early stages of the anodization process Al^{3+} ions migrate from the metal across the metal/oxide interface into the forming oxide layer [40]. Meanwhile, O^{2-} ions formed from water at the oxide/electrolyte interface travel into the oxide layer. During this stage approximately 70% of the Al^{3+} ions and the O^{2-} ions contribute to the formation of the barrier oxide layer [41], the remaining Al3+ ions are dissolved into the electrolyte. This condition has been shown to be the prerequisite for porous oxide growth, in which the Al-O bonds in the oxide lattice break to release Al^{3+}+ ions [42]. During the oxide formation the barrier layer constantly regenerates with further oxide growth and transforms into a semi-spherical oxide layer of constant thickness that forms the pore bottom, as shown in Figure 4.

Figure 4. Schematic of the pore formation mechanism in an acidic electrolyte.

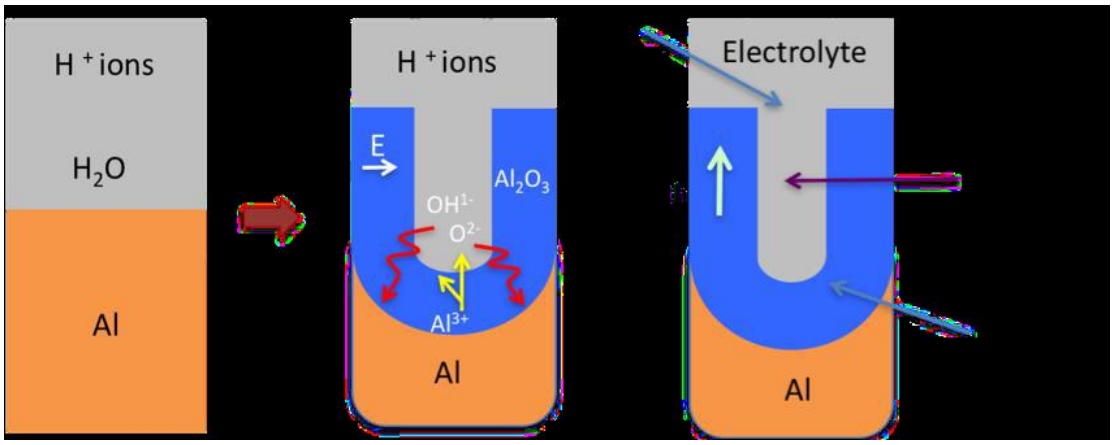

The steady state growth results from the balance between the field-enhanced oxide dissolution at the oxide/electrolyte interface at the base of the hemispherical shaped pores where the electric field is high enough to propel the Al^{3+} ions through the barrier layer and the oxide growth at the metal/oxide interface resulting from the migration of O^{2-} and OH^{-} ions into the pore base oxide layer, see Figure 5. This also explains the dependence of the size of the pore diameter to the electric field produced by the anodizing voltage. It should also be noted that the electric field strength in the pore walls is too small to make any significant contribution to the flow of ions.

The oxidation takes place over the entire pore base and the resulting oxide material grows perpendicular to the surface, neighboring pore growth prevents

growth in any other direction. The vertical growth of the pore wall creates a columnar structure with a high aspect ratio that contains a central circular channel. This channel extends from the base of the pore to the surface of the oxide layer. This upward growth of the pore wall was recently investigated by Garcia-Vergara *et al.* in which a tungsten tracer was placed into an initial oxide layer formed by an initial anodization step [36]. During the next stage of anodization, the position of the tracer was monitored and found to travel from the metal/oxide interface of the barrier layer located at the base of the pore towards the growing wall structure. This flowing motion of the tracer was credited to the mechanical stresses being generated by the continued formation of new oxide within the pore base and the repulsive forces set up between neighboring pores during the growth of the wall structure. These forces resulted from the volume expansion (by a factor of 2) during the oxidation of Al to alumina. This volumetric expansion factor results from the difference in the density of Al in alumina (3.2 g cm−2) and that of metallic Al (2.7 g cm−2). This volumetric oxide expansion at the metal/oxide interface also contributes to the hemispherical shape of the pore base. However, under normal experimental conditions, the volumetric expansion factor is less than 2. This is due to the hydration reaction that occurs at the oxide/electrolyte interface which results in the dissolution and thinning of the oxide layer.

Figure 5. Schematic of ion movement during pore formation.

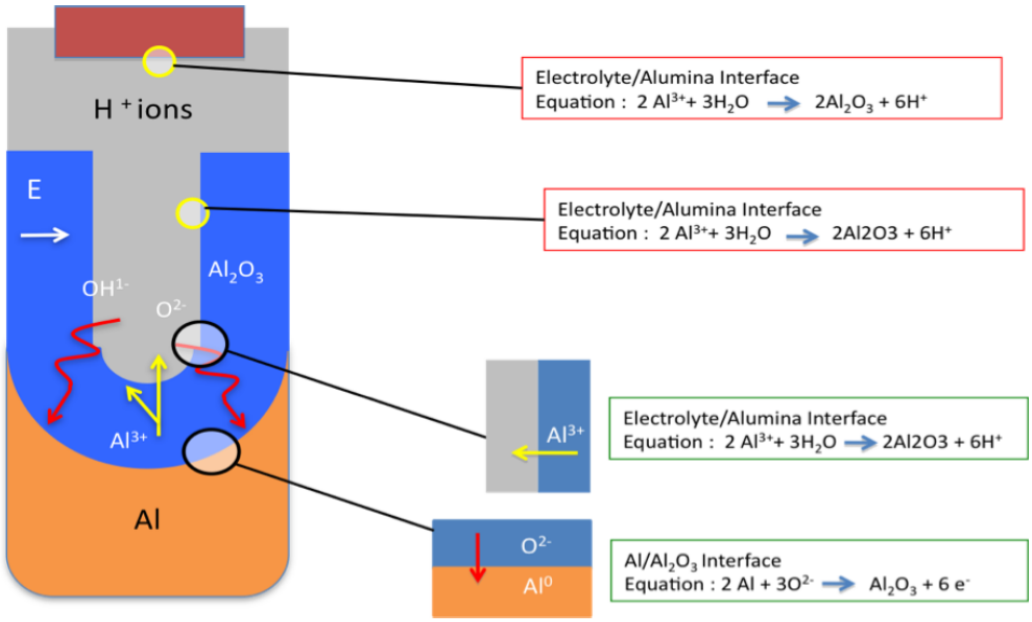

The mechanical stress generated at the metal/oxide interface during the formation of the oxide layer also influences the self-ordering of the developing pores.

During the initial stage of anodization, the pores nucleate and develop randomly over the Al surface. As the anodizing time increases, the growth of the oxide layer progresses and characteristic pore patterns begin to immerge. The pore patterns continue to develop and become more ordered, with some self-adjustment of the pore configurations taking place [43]. Eventually, the number of various pore arrangements decrease until a single, long-range ordered pore structure is formed. The ideal structure consists of a densely packed hexagonal array of ordered pores of uniform size [44] see Figure 6. The pore density can range from 108 to 1012 pores per cm2 depending upon the preparation parameters [42,45].

Figure 6. (**A**) Schematic of the ideal densely packed hexagonal array of pores; (**B**) Actual cross sectional view of a typical synthesized AAO membrane**.**

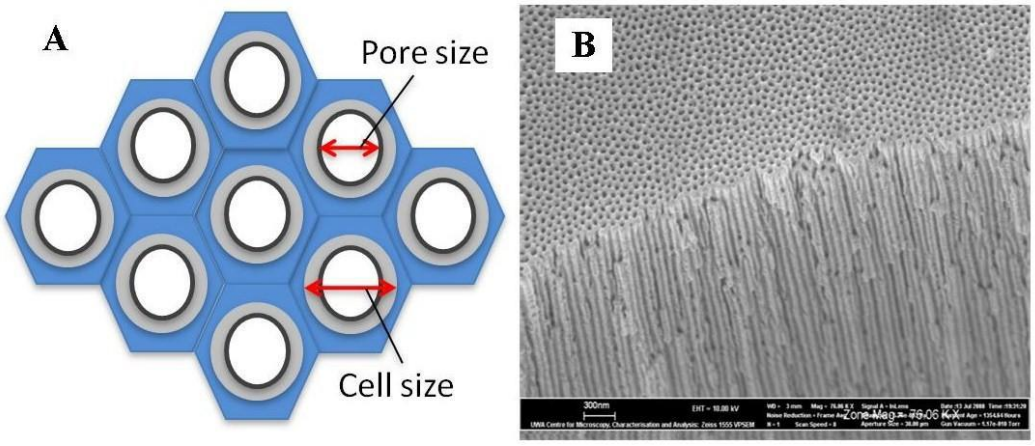

The image reveals a self ordered structure that has no densely packed pore arrangement or any long range order in the oxide layer.

Figure 7. Scanning Electron Microscopy (SEM) image of self ordered pore array‘s in an aluminum oxide layer.

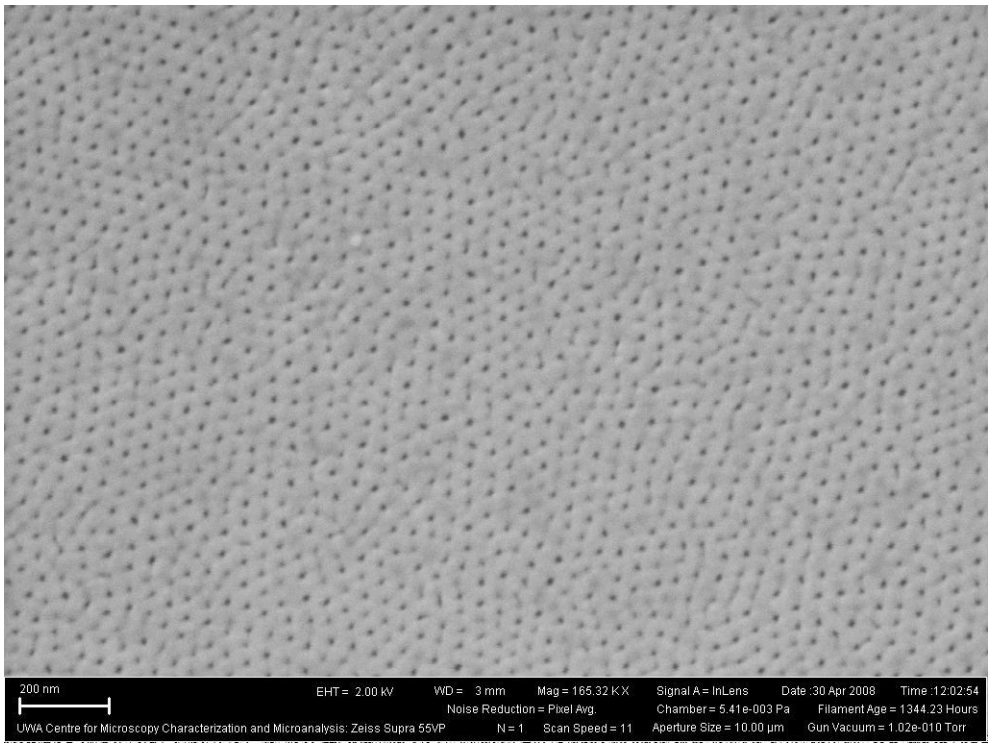

In addition, the naturally occurring self-ordering of the pores has also limited the size of both the pore and cell produced during anodization process. Studies have shown that the cell size is generally constrained to around 100 nm. However, AAO membranes used in optical devices, particularly in the infrared region of the spectrum require larger cell sizes. These larger cell sizes are possible by controlling the anodization parameters of electrolyte, electrolyte concentration, temperature, current density and anodizing voltage. For example, one procedure that is used to increase the pore/cell size uses phosphoric acid and a steady state voltage of 195 V, the result is a self ordered AAO membrane with cell sizes around 500 nm [4]. Further studies into the growth kinetics of porous layers formed by anodization in phosphoric acid under galvanostatic conditions have shown that the rate of growth of the oxide layer increases with increasing current density. At low current densities, (7.5 mA/cm2) the increase in the growth rate is proportional to the temperature. While at higher current densities, (17.5 mA/cm2) increasing the temperature has no effect on the growth rate. These studies have also revealed that the anodization time influenced the porosity of the oxide layer and that the layer growth and the oxide dissolution rate controlled the layers morphology [42,46].

CHAPTER 3

MATERIALS AND METHODS

Al (Mn = 0.10%, Si = 0.10% and Fe = 0.10%) of thickness 0.80 mm, 1.0 cm in width and 5.0 cm in length for thermometric method, was degreased before each run using a solution containing Na_2CO_3 (25 g / dm^3), Na_3PO_4 (25 g / dm^3) and wetting agent (synthetic detergent with the active ingredient dodecylbenzene sulphonate) (10 g / dm^3) for 5 minutes at 85.0^oC, then washed with distilled water and dipping in a pickling solution (4 M HCl) for one minute followed by hot and cold distilled water.

An DC treatment (Fig. 1) of specimens was carried out using power supply and two identical Al electrodes 3.0 cm apart were immersed in 90.0 cm^3 of 1 M sodium carbonate solution, oxalic acid, phosphoric acid or sulphuric acid. Also, the effect of different variables (applied DC voltages, concentration of sodium carbonate solution and the anodization time) on the anodization of Al in commercial low-cost salt compound was studied.

The microphotographs of the anodic film formed on the surface of Al were made using a scanning electron microscope JEOL Model JSM-T 200.

The structure and composition of the anodic film formed on the surface of Al was examined using x-ray diffraction technique. X-ray diffractometer Model JSX-60PA JEOL, LTD, was used with nickel filter and copper radiation (λ = 1.54184 nm).

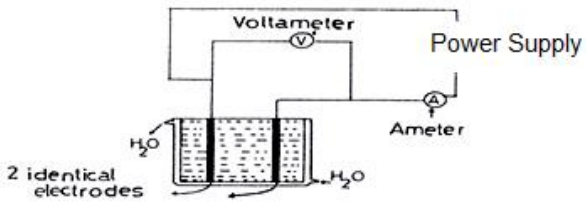

Anodization Cell

Figure 8

The cathodic and anodic behavior of Al in 1 M of Na_2CO_3 solution at 25.0 ^oC was investigated using Potentiostat/Galvanostat Model 273A (EG, G Princeton Applied Research).

The range of study was from - 0.25 V to + 0.5 V versus open circuit potential (O.C.P.). The effect of the scanning rate on the polarization of Al in the salt was studied also.

In thermometric determination (Fig. 9) the specimens were dipped in HCl solution placed in closed glass cell. The rise of temperature by time was followed using a 100^{o}C thermometer. All experiments were carried out in adiabatic conditions as the apparatus was kept in a Dewier flask, which is fixed in an air thermostat at 25.0^{o}C.

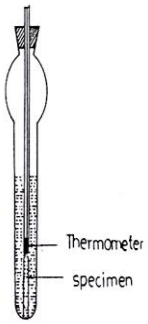

Thermometric Cell

Figure 9

The relations (T-τ) and quantitative treatment of data:

Figures 9 as example show the relations T-τ (thermometric method) of Al anodized at different voltages and untreated Al specimens in 2M HCl solution. These figures show a distinct nonlinear behavior at first portion, and then passing through a linear one after a certain activation period. The transition from the nonlinear to linear character is mainly attributed to the leveling interaction of many factors, namely change in HCl concentrations, appearance and accumulation of Al ions, the state of the surface and the temperature together on the measured value (T). The results obtained for each type of experiment were investigated based on the following relations:

(i) Linear regression : $\tau = A + B(\Delta T)$ (1)

(ii) Logarithmic regression: $\tau = A + B \log (\Delta T)$ (2)

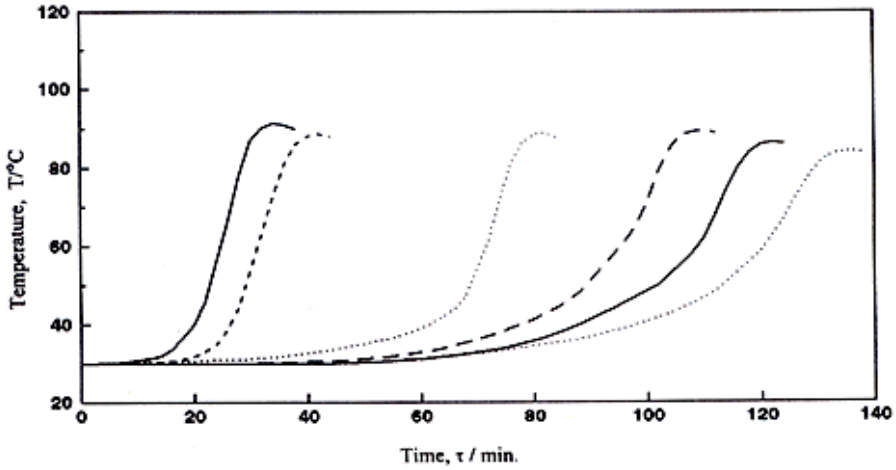

Untreated Al	40V	60V	80V	100V	120V
_____	--------	……	_ _ _ _ _	_____	……..

Figure 10. T-τ curves for Al, anodized in 1M sodium carbonate at different DC voltage for 20 min. at 25 ^{o}C, in ??? cm3 HCl at initial temperature 30 ^{o}C.

where τ is the time and ΔT is the rise in temperature in the thermometric method. The data obtained were treated using regression analysis. Tables 1 and 2 indicate example for the data treatment of untreated and anodized Al (at 15 V) curves for each method during the dissolution of specimen in the HCl. The values of A and B, the constants in eqs.1 and 2 together with r -the correlation coefficient, t -the student criterion (t test) and α- the level of significance are reported in these Tables. It is quite clear from these Tables that the method can be expressed successively by a linear equation for the clear linear portion in the T-τ relationship and by logarithmic equation for the first nonlinear portion.

Table 1. Values of A, B, r, t and α for thermometric measurements during the dissolution of untreated Al and Al , anodized in 1 M sodium carbonate solution at 40 volt for 20 min. at 30.0°C, in 100 mL 3 M HCl solution at initial temperature t_o=30.0°C

Applied voltage		Logarithmic regression $\tau = A+B \log (\Delta T)$	Linear regression $\tau = A+ B(\Delta T)$
Untreated Al	A	7.20	13.4
	B	6.48	0.143
	r	0.987	0.982
	t	15.0	7.35
	α	0.00-α -0.001	0.01-α -0.02
40 volt	A	50.8	85.8
	B	24.4	0.338
	r	0.986	0.994
	t	20.5	18.2
	α	0.00-α -0.001	0.00-α -0.001

[(A) Constant term. (B) Regression coefficient. (r) Correlation coefficient.

(t) Student criterion. (α) Level of significance.]

So the relation could be expressed over a wide range of the clear nonlinear portion by the empirical formula: $\tau = A + B \log (\Delta T)$ (3)

where A and B are constants, ΔT=T-To at time τ. A, times needed for the temperature to reach ΔT=1°C, while B is the time required for raising the temperature from 26.0°C to 35.0°C.

At the same time the T-τ relation can be expressed satisfactorily for the clear linear portion by the empirical formula: $\tau = A^{\bullet} + B^{\bullet} \Delta T$ (4)

where $A^{\bullet}$ and $B^{\bullet}$ are constants, $A^{\bullet}$ is the time at intersection of the extended linear portion, while $B^{\bullet}$ is the time needed for raising the temperature by 1.00°C

during the linear portion. In the present work the τ_L which is the time needed to start the linear portion used to compare between the obtained results.

CHAPTER 4

RESULTS AND DISCUSSION

4.1. The effect of electrolyte type:

It is quite clear from Figure 10 that's the type of electrolyte affect the anodization and in turn the dissolution resistant of the anodized Al. It's obvious that the sulphuric acid has more dissolution resistance. May be due to that the Electrolytes are composed of less concentrated acids tend to produce oxide coatings that are harder, thicker, less porous and more wear resistant than those composed of higher concentrated acids [30]. This means that the sulphuric acid made more porous, which increase the surface area and in turn the corrosion resistance increases.

When the current is flowing in the cell the following sequence of events is believed to occur[47-50]. Sulphuric acid begins to decompose, the hydrogen ions moving to the cathode where they are reduced to hydrogen gas:

$$2H^+ + 2e^- \rightarrow H_2(g) \quad (5)$$

$$Al \rightarrow Al^{3+} + 3e- \quad (6)$$

$$2Al^{3+} + 3O^{2-} \rightarrow Al_2O_3 \quad (7)$$

$$2Al^{3+} + 3OH^- \rightarrow Al_2O_3 + 3H^+ \quad (8)$$

• For which the overall process is:

$$2Al + 3H_2O \rightarrow Al_2O_3 + 6H^+ + 6e- \quad (9)$$

The sulphate ions also play some part as the oxide coating contains 12 - 15% sulphate ions. It is suggested that the sulphate ions facilitate the movement of hydrogen ions reducing the cell voltages required.

The etching reaction:

$$2Al + 2NaOH + 2H_2O \rightarrow 2NaAlO_2 + 4H_2 \quad (10)$$

• Dissolution of the aluminate:

$$NaAlO_2 + H_2O \rightarrow NaOH + Al(OH)_3 \quad (11)$$

• Dehydration of the solid hydroxide:

$$2Al(OH)_3 \rightarrow Al_2O_3 + 3H_2O \quad (12)$$

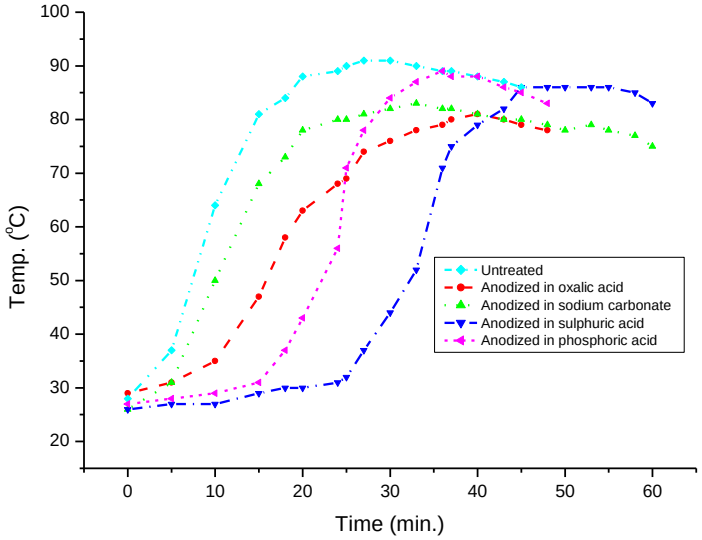

Figure 11. T-τ curves for Al, anodized in different electrolyte type at 15 DC voltage for 15 min. at 25 ^{o}C, in HCl at initial temperature 25 ^{o}C.

4.2. The effect of applied DC voltage:

From the obtained results, Figure 10, one may come to the general conclusion that by applying DC voltage in the range 15-120 V an improvement in the surface properties of Al was observed by increasing of voltage value. Meanwhile, the use of 15 V brings about very little improvement in the dissolution resistance. Applied DC voltages higher than 15 V were found to give relatively high an improvement in the dissolution resistance with respect to the anodization at 15 V. This behavior is expected at higher values of voltage. This could be attributed to the varying of sodium carbonate velocity according to the applied potential, so, transport number will affect. At lower values of potential, zone of growth of the oxide layer is expected to be located in the oxide/electrolyte interface, giving rise to dissolution resistance porous oxide film (Figs. 12). While, the application of high voltage is capable of forcing the unions to move faster, and at the same time the zone of growth is thus pushed backward inside the oxide layer itself. As a result partially defected oxide film is formed and the dissolution resistance of Al becomes a little worse.

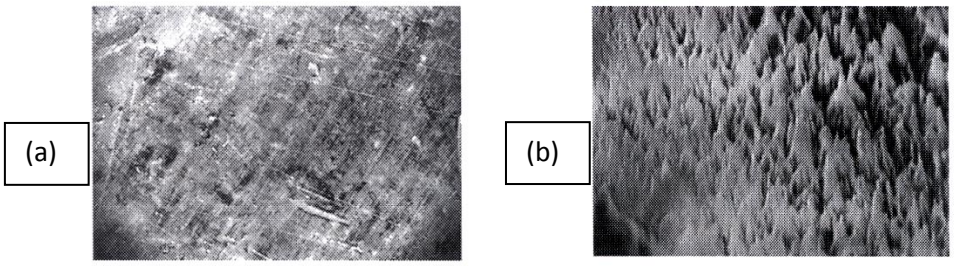

Figure 12. Photographic of anodic film on Al, anodized in (a) 1 M sodium carbonate solution at 40 V for 15 min. at 25 ^{o}C (b) untreated. (Magnification of 1500x)

4.3. X-ray diffraction analysis:

Two forms of anhydrous Al_2O_3, namely α- Al_2O_3 and γ- Al_2O_3 are known. In α- Al_2O_3 the oxide ions form a hexagonally close-packed array and the aluminum ions are distributed symmetrically among the octahedral interstices. The γ-Al_2O_3 structure is sometimes regarded as "defect" spinel structure. α- Al_2O_3 is stable at high temperatures, very hard and resistant to hydration and attack by acids. X-ray investigation (Fig.13) revealed that the formed film on anodized Al is α- Al_2O_3 with traces of γ- Al_2O_3. Also, it is obvious, that the α- Al_2O_3 content decrease in untreated than in anodized Al. For the anodized specimens γ- Al_2O_3 content was found to decrease as the volt increase.

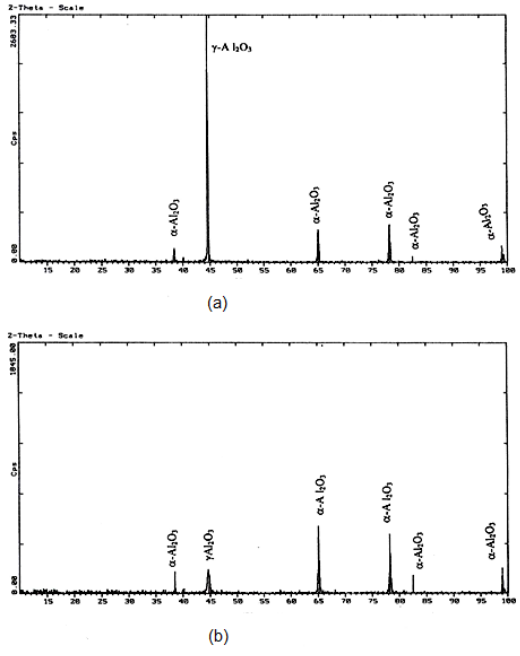

Figure 13. X-ray diffraction for different specimens: (a) Untreated Al. (b) Al anodized in 1 M sodium carbonate solution at 40 V for 15 min. at 25 ^{o}C.

4.4. The anodic and cathodic behavior:

The anodic curves of potentiodynamic study were found to be distinctly more sensitive towards scanning rate variations rather than the cathodic ones. This behavior is quite explainable on the basis of the diffusion control, which is almost absent in the cathodic process (hydrogen evolution) and on the contrary strongly exists in the anodic process (anodization of Al).

Fig. 14 shows that with increasing scan rate (ranging 5 mV/s – 50 mV/s) the passive current increased. This may be explained on the basis of the film thickness.

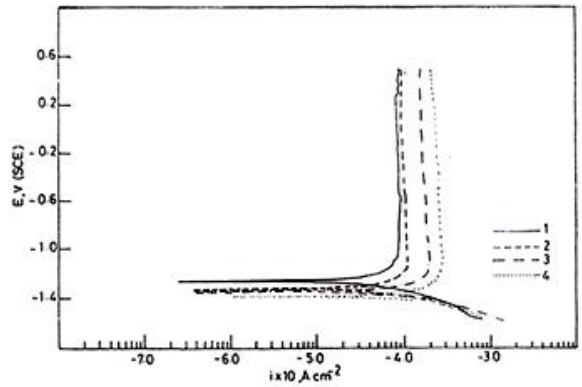

Anodic and cathodic potentiodynamic polarization curves for Al in 0.1 M sodium carbonate solution at different scanning rate.
1- 5 mV/s. 2- 10 mV/s. 3- 25 mV/s. 4- 50 mV/s.

Figure 14

It is quite clear from Fig.15 that the passive current for treating Al is less than untreated ones due to the formation of oxide films.

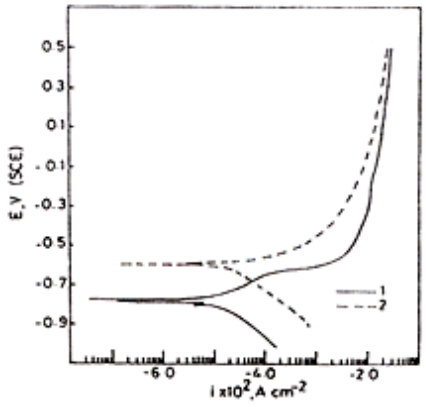

Anodic and cathodic potentiodynamic polarization curves for Al, anodized in 0.1 M sodium carbonate solution at 0.5 V for 20 min., in 0.1 M HCl.
1- Untreated Al. 2- Treated Al.

Figure 15

CHAPTER 5
CONCLUSION

Anodizing aluminum was carried out using direct current to study firstly the effect of electrolyte type using different acids and sodium carbonate on the corrosion resistance of AAO formed. The obtained results show that the anodization in sulphuric acid was the best one. Secondly, the effect of applied voltages on the anodization of Al in commercial low-cost salt compound (sodium carbonate solution) for protective applications was also part of this work. In general the dissolution resistance rate increases with increasing DC voltage.

REFERENCES

1.Smallman, R.E.; Bishop, R.J. *Modern Physical Metallurgy and Materials Engineering*, 6th ed.; Butterworth Heinemann: Oxford, UK, 1999; Chapter 9.

2. Anodisation of aluminium: New applications for a common technology. Nano Wizard Application Report, Cambridge, UK, September 2003.

3. HM Wire International Inc. Bengough-Stuart Process. Available online: http://www.litz-wire.com (accessed on 29 June 2010).

4. Masuda, H.; Yada, K.; Osaka, A. Self-ordering of cell configuration of anodic porous alumina with large-size pores in phosphoric acid solution. *Jpn. J. Appl. Phys*. **1998**, *37*, L1340-L1342.

5. Ramakrishna, S.; Ramalingam, M.; Sampath Kumar, T.S.; Soboyejo, W.O. Recent trends in biomaterials. In *Biomaterials a Nano Approach*, 1st ed.; CRC Press: Boca Raton, FL, USA, 2010, pp. 22-27.

6. Greco, R.S.; Prinz, F.B.; Smith, R.L. *Nanoscale Technology in Biological Systems*, 1st ed.; CRC Press: Boca Raton, FL, USA, 2005.

7. Lines, M.G. Nanomaterials for practical functional uses. *J. Alloys Componds* **2008**, *449*, 242-245.

8.US Geological Survey. Available online: http://minerals.usgs.gov/minerals/pubs/commodity/ aluminium (accessed on 15February 2011).

9. Dignam, M.J. Oxide films on aluminium. *J. Electrochemical. Soc.* **1962**, *109*, 184-191.

10. Thompson, G.E. TALAT Lecture 5101: Surface characteristics of aluminium and aluminium alloys. European Al Ass, 30 April 2010. Available online: http://core.materials.ac.uk/search/ detail.php?id=2243 (accessed on 7 January 2011).

11. Verwey, E.J.W. Electrolytic conduction of a solid insulator at high fields for the formation of the anodic oxide film on aluminium. *Physica* **1935**, *2*, 1059-1063

12. Diggle, J.W.; Downie, T.C.; Goulding, C.W. Anodic oxide films on aluminium. *Chem. Rev.* **1969**, *69*, 365-405.

13. Thompson, G.E. Porous anodic alumina: Fabrication, characterisation and application. *Thin Solid Films* **1997**, *297*, 192-201.

14. Keller, F.; Hunter, M.S.; Robinson, D.L. Structural features of oxide coatings on aluminium. *J. Electrochemical. Soc.* **1953**, *100*, 411-419.

15. Morrison, S.R. *Electrochemistry at Semiconductor and Oxidized Metal Electrodes*; Plenum: New York, NY, USA, 1980; Chapter 8, pp. 306-318.

16. Uchi, H.; Kanno, T.; Alwitt, R.S. Structural features of crystalline anodic alumina films. *J. Electron. Soc. Vol.* **2001**, *148*, B17-B23.

17. Brace, A.W.; Sheasby, P.G. *The Technology of Anodising Aluminium*; Technicopy Limited: London, UK, 1979.

18. Surface characteristics of aluminium and aluminium alloys. Available online: http://www.eaa.net/eaa/education/TALAT (accessed on 20 August 2010).

19.Zaraska, L.; Sulka, G.D.; Szeremeta, J.; Jaskula, M. Porous anodic alumina formed by anodisation of aluminium alloy (AA1050) and high purity aluminium. *Electrochim. Acta* **2010**, *55*, 4377-4386.

20.Alwitt, R.S. *Anodizing*; Electrochemistry Encyclopaedia Boundary Technologies Inc: Northbrook, IL, USA, 2002.

21.Li, F.; Zhang, L.; Metzger, R.M. On the growth of highly ordered pores in anodized aluminium oxide. *Chem. Mater* **1998**, *10*, 2470-2480.

22. Jessensky, O.; Muller, F.; Gosele, U. Self-organized formation of hexagonal pore arrays in anodic alumina. *Appl. Phys. Lett*. **1998**, *72*, 1173-1175.

23. Jessensky, O.; Muller, F.; Gosele, U. Self-organised formation of hexagonal pore structures in anodic alumina. *J. Electrochem. Soc.* **1998**, *145*, 3735-3740.

24. Li, F.; Zhang, L.; Metzger, R.M. On the growth of highly ordered pores in anodized aluminium oxide. *Chem. Mater*. **1998**, *10*, 2470-2480.

25. Li, A.P.; Muller, F.; Birner, A.; Nielsch, K.; Gosele, U. Polycrytalline nanopore arrays with hexagonal ordering on aluminium. *J. Vac. Sci. Technol. A* **1999**, *17*, 1428-1431.

26. Li, A.P.; Muller, F.; Birner, A.; Nielsch, K.; Gosele, U. Hexagonal pore arrays with a 50–420 interpore distance formed by self-organisation in anodic alumina. *J. Appl. Phys*. **1998**, *84*, 6023-6026.

27. Zhang, L.; Cho, H.S.; Li, F.; Metzger, R.M.; Doyle, W.D. Cellular growth of highly ordered porous anodic films on aluminium. *J. Mater. Sci. Lett.* **1998**, *17*, 291-294.

28. Hou, K.; Tu, J.P.; Zhang, X.B. Preparation of porous alumina film on aluminium substrate by anodisation in oxalic acid. *Chin. Chem. Lett.* **2002**, *13*, 689-692.

29. Kim, Y.S.; Pyun, S.I.; Moon, S.M.; Kim, J.D. The effects of applied potential and pH on the electrochemical dissolution of the barrier layer in porous anodic oxide film on pure aluminium. *Corros. Sci.* **1996**, *38*, 329-336.

30.O'Sullivan, J.P.; Wood, G.C. Nucleation and growth of porous anodic films on aluminium. *P Roy. Lond. A Mat.* **1970**, *A317*, 511-543.

31.O'Sullivan, J.P.; Wood, G.C. Nucleation and growth of porous anodic films on aluminium. *P Roy. Lond. A Mat.* **1970**, *A317*, 511-543.

32.Hoar, T.P.; Mott, N.F. A mechanism for the formation of porous anodic oxide films on aluminium. *J. Phys. Chem. Solid*. **1959**, *9*, 97-99.

33.Thompson, G.E.; Furneaux, R.C.; Wood, G.C.; Richardson, J.A.; Goode, J.S. Nucleation and growth of porous anodic films on aluminium. *Nature* **1978**, *272*, 433-435.

34.Vrublevsky, I.; Jagminas, A.; Schreckenbach, J.; Goedel, W.A. Electronic properties of electrolyte/anodic alumina junction during porous anodizing. *Appl. Surf. Sci.* **2007**, *253*, 4680-4687.

35.Thompson, G.E.; Xu, Y.; Skeldon, P.; Shimizu, K.; Han, S.H.; Wood, G.C. Anodic oxidation of aluminium. *Philos. Mag. Part B* **1987**, *55*, 651-667.

36. Garcia-Vergara, S.J.; Iglesias-Rubianes, L.; Blanco-Pinzon, C.E.; Skeldon, P.; Thompson, G.E.; Campestrini, P. Mechanical instability and pore generation in anodic alumina. *P. Roy Soc. Lond. A Mat.* **2006**, *462*, 2345-2358.

37.Hoar, T.P.; Yahaloom, J. The initiation of pores in anodic oxide films formed on aluminium in acid solutions. *J. Electrochem. Soc.* **1963**, *110*, 614-621.

38.Patermarakis, G. The origin of nucleation and development of porous nanostructure of anodic alumina films. *J. Electroanal. Chem.* **2009**, *635*, 39-50.

39.Habazaki, H.; Shimizu, K.; Skeldon, P.; Thompson, G.E.; Wood, G.C.; Zhou, X. Nanoscale enrichments of substrate elements in the growth of thin oxide films. *Corros. Sci.* **1997**, *39*, 731-737.

40. Patermarakis, G. Development of a theory for the determination of the composition of the anodising solution inside the pores during the growth of porous anodic Al2O3 films on aluminium by a transport phenomenon analysis. *J. Electroanal. Chem.* **1998**, *447*, 25-41.

41. Palbroda, E. Aluminium porous growth—II on the rate determining step. *Electrochim. Acta* **1995**,*40*, 1051-1055.

42. Shawaqfeh, A.T.; Baltus, R.E. Fabrication and characterization of single layer and muti-layer anodic alumina membrane. *J. Membrane Sci*. **1999**, *157*, 147-158.

43. Ono, S.; Saito, M.; Asoh, H. Self ordering of anodic porous alumina formed in organic acid electrolytes. *Electrochem. Solid-State Lett.* **2004**, *7*, B21-B24.

44. Jessensky, O.; Muller, F.; Gosele, U. Self-organised formation of hexagonal pore structures in anodic alumina. *J. Electrochem. Soc.* **1998**, *145*, 3735-3740.

45. Prasad, S.; Quijano, J. Development of nanostructured biomedical micro-drug testing device based on in situ cellular activity monitoring. *Bioelectronics* **2006**, *7*, 1219-1229.

46. Ghorbani, M.; Nasirpouri, F.; Iraji zad, A.; Saedi, A. On the growth sequence of highly ordered nano-porous anodic aluminium oxide. *Mater. Des.* **2006**, *27*, 983-988.

47. Brace, A.W. and Sheasby, P.G.; *The Technology of Anodising Aluminium*; Technicopy

48. Fahy, F.W.; *Anodised Aluminium - Its Assessment by Accelerated Corrosion*; Paper presented at Symposium of Anodised Aluminium, 15th February 1979

49. Hsieh An Kong, S.; *Colouring Anodised Aluminium - A Review*; Metal Finishing; October 1981

50.Wright, G.A.; *Recent Research on Anodic Films on Aluminium*; Paper presented at Symposium on Anodised Aluminium; 15th February 1979.